Harmonic Resonance Mode Analysis

CONFERENCE PAPER *in* IEEE TRANSACTIONS ON POWER DELIVERY · JULY 2005

Impact Factor: 1.73 · DOI: 10.1109/PES.2005.1489238 · Source: IEEE Xplore

4 AUTHORS, INCLUDING:

Zhenyu Huang
United International College
90 PUBLICATIONS **822** CITATIONS

SEE PROFILE

Harmonic Resonance Mode Analysis

Wilsun Xu, *Senior Member, IEEE*, Zhenyu Huang, *Member, IEEE*, Yu Cui, and Haizhen Wang

***Abstract*—Harmonic resonance often manifests as high harmonic voltages in a power system. It was found that such resonance phenomenon is associated with the singularity of the network admittance matrix. The singularity, in turn, is due to the fact that one of the eigenvalues of the matrix approaches zero. By analyzing the characteristics of the eigenvalue, one can find useful information on the nature and extent of the resonance. The objective of this paper is to present our findings on this interesting subject. Based on the results, a technique called Resonance Mode Analysis is proposed. Analytical and case study results have confirmed that the proposed method is a valuable tool for power system harmonic analysis.**

***Index Terms*—Eigenvalue, harmonic resonance, harmonics, modal analysis, power quality.**

I. Introduction

HARMONIC resonance is one of the main consequences of harmonics in power systems. Many harmonic-related equipment problems can be traced to the phenomenon [1]. Although the cause of harmonic resonance is well understood, tools available to analyze the phenomenon are very limited. Frequency scan analysis is probably the only viable method at present to identify the existence of resonance and to determine the resonance frequency [2]. Unfortunately, the tool cannot offer additional information needed to solve the problem effectively.

Harmonic resonance is caused by the energy exchange between capacitive elements and inductive elements in a system. Since a power system contains numerous inductive and capacitive elements, the phenomenon of harmonic resonance can become quite complicated. It would be very useful to have a tool that can "untangle" the complex interactions among the energy storage elements and can reveal the true "culprits" that lead to a particular resonance problem. For example, answers to the following questions will greatly help one to find solutions to mitigate harmonic resonance problems:

- Which bus can excite a particular resonance more easily?
- Where can the resonance be observed more easily?
- What components are involved in the resonance?
- How far can the resonance propagate in a system?
- Do the resonance phenomena observed at difficult buses originate from the same cause?

Manuscript received December 18, 2003; revised April 17, 2004. This work was supported by the Natural Science and Engineering Research Council of Canada. Paper no. TPWRD-00642-2003.

W. Xu is with the University of Alberta, Edmonton, AB T6G 2G7, Canada. He is also with Shandong University, Jinan City, Shandong 250100 China (e-mail: wxu@ece.ualberta.ca).

Z. Huang is with the Pacific Northwest National Laboratory, Richland, WA 99352 USA (e-mail: zhenyu.huang@pnl.gov).

Y. Cui and H. Wang are with the University of Alberta, Edmonton, AB T6G 2G7, Canada (e-mail: yucui@ece.ualberta.ca).

Digital Object Identifier 10.1109/TPWRD.2004.834856

The objective of this paper is to present a method that has the potential to solve some of the above problems. Over the years, we observed that (parallel) harmonic resonance is related to the presence of large elements in the inverted network admittance matrix $[Y]$. In the extreme case where the $[Y]$ matrix becomes singular, the elements of $[Y]^{-1}$ could become infinity and very high voltages could be produced. This is, in fact, the most serious form of parallel resonance. We further reasoned that a singular $[Y]$ matrix occurs only when one of the eigenvalues of the matrix is zero. This zero eigenvalue could be the real source of the resonance phenomenon. It may well define the mode of harmonic resonance. With this understanding, the analysis of harmonic resonance can be transformed into a study of critical resonance modes. A modal (or eigen) analysis method is thus proposed in this paper for investigating the harmonic resonance problem.

This paper is organized as follows. The concept of harmonic resonance modes is introduced in Section II. Characteristics of harmonic resonance modes are discussed in Section III. In Section IV, case studies are presented to demonstrate the unique information that can be provided by the Resonance Mode Analysis (RMA) technique. The conclusions are summarized Section V along with discussions on how to conduct resonance mode analysis.

II. Concept of Resonance Modes

Imagine a system experiencing a sharp parallel resonance at frequency f according to the frequency scan analysis. This means that some elements of the voltage vector calculated from the following equation have large values at f.

$$[V_f] = [Y_f]^{-1}[I_f] \tag{1}$$

where $[Y_f]$ is the network admittance matrix at frequency f. $[V_f]$ is the nodal voltage and $[I_f]$ the nodal current injection respectively. $[I_f]$ has only one entry that has a value of 1.0 p.u. The other elements are 0. To simplify notation, the subscript f will be omitted hereinafter.

A sharp harmonic resonance means that some nodal voltages are very high. This will occur when the $[Y]$ matrix approaches singularity. To investigate how the $[Y]$ matrix approaches singularity is therefore an attractive way to analyze the problem. The well-established theory of eigen-analysis can be applied for this purpose. According to the theory [3], the Y matrix can be decomposed into the following form:

$$[Y] = [L][\Lambda][T] \tag{2}$$

where $[\Lambda]$ is the diagonal eigenvalue matrix, $[L]$ and $[T]$ are the left and right eigenvector matrices respectively. $[L] = [T]^{-1}$. Substituting (2) into (1) yields

$$[V] = [L][\Lambda]^{-1}[T][I]$$

or

$$[T][V] = [\Lambda]^{-1}[T][I]. \tag{3}$$

Defining $[U] = [T][V]$ as the modal voltage vector and $[J] = [T][I]$ as the modal current vector respectively, the above equation can be simplified as

$$[U] = [\Lambda]^{-1}[J]$$

or

$$\begin{bmatrix} U_1 \\ U_2 \\ \dots \\ U_n \end{bmatrix} = \begin{bmatrix} \lambda_1^{-1} & 0 & 0 & 0 \\ 0 & \lambda_2^{-1} & 0 & 0 \\ 0 & 0 & \dots & 0 \\ 0 & 0 & 0 & \lambda_n^{-1} \end{bmatrix} \begin{bmatrix} J_1 \\ J_2 \\ \dots \\ J_n \end{bmatrix}. \tag{4}$$

The inverse of the eigenvalue, λ^{-1}, has the unit of impedance and is named modal impedance (Z_m). From (4), one can easily see that if $\lambda_1 = 0$ or is very small, a small injection of modal 1 current J_1 will lead to a large modal 1 voltage U_1. On the other hand, the other modal voltages will not be affected since they have no 'coupling' with the mode 1 current. In other words, one can easily identify the 'location' of resonance in the modal domain. The implication is that the resonance actually takes place for a specific mode. It is not related to or caused by a particular bus injection. We therefore call the smallest eigenvalue the critical mode of harmonic resonance and its left and right eigenvectors the critical eigenvectors.

The modal current J_1 is a linear projection of the physical currents in the direction of the first eigenvector as follows:

$$J_1 = T_{11}I_1 + T_{12}I_2 + T_{13}I_3 + \dots + T_{1n}I_n.$$

It can be seen that if T_{13} has the largest value, nodal current I_3 will have the largest contribution to the modal 1 current. As a result, bus 3 is the location where the modal 1 resonance can be excited most easily. On the other hand, if $T_{13} = 0$, current I_3 will not be able to excite the mode no matter how large the current is. The values of the critical eigenvector $[T_{11}, T_{12}, \dots T_{1n}]$ can therefore be used to characterize the significance of each nodal current to excite the modal 1 resonance.

The physical nodal voltages are related to the modal voltages by equation $[V] = [L][U]$ as follows

$$\begin{bmatrix} V_1 \\ V_2 \\ \dots \\ V_n \end{bmatrix} = \begin{bmatrix} L_{11} \\ L_{21} \\ \dots \\ L_{n1} \end{bmatrix} U_1 + \begin{bmatrix} L_{12} \\ L_{22} \\ \dots \\ L_{n2} \end{bmatrix} U_2 + \dots + \begin{bmatrix} L_{1n} \\ L_{2n} \\ \dots \\ L_{nn} \end{bmatrix} U_n$$
$$\approx \begin{bmatrix} L_{11} \\ L_{21} \\ \dots \\ L_{n1} \end{bmatrix} U_1.$$

The above approximation is possible since U_1 has a value much larger than other modal voltages. This equation reveals that the contribution of the U_1 voltage to the physical voltages can be characterized using the vector $[L_{11}, L_{21}, \dots L_{n1}]^{\mathrm{T}}$. If L_{31} has the largest value, bus 3 will also have the largest value. This implies that bus 3 is the location where the modal 1 resonance can be most easily observed. If $L_{31} = 0$, the nodal 3 voltage will not be affected by the modal 1 voltage.

In summary, the critical right eigenvector has the potential to characterize the (locational) excitability of the critical mode and the critical left eigenvector can represent the (locational) observability of the critical mode. The bus with the largest right eigenvector element is the bus possessing the highest excitability for the mode and that with the largest left eigenvector element is the one possessing the highest observability. Excitability can also be understood as a form of controllability as buses with the highest excitability are the most effective locations to inject signals to cancel harmonics.

It is possible to combine the excitability and observability into a single index according to the theory of selective modal analysis [4], as follows:

$$[V] = [L][\Lambda]^{-1}[T][I] = [L] \begin{bmatrix} \lambda_1^{-1} & 0 & 0 & 0 \\ 0 & \lambda_2^{-1} & 0 & 0 \\ 0 & 0 & \dots & 0 \\ 0 & 0 & 0 & \lambda_n^{-1} \end{bmatrix} [T][I]$$
$$\approx \begin{bmatrix} L_{11} & L_{12} & \dots & L_{1n} \\ L_{21} & L_{22} & \dots & L_{2n} \\ \dots & \dots & \dots & \dots \\ L_{n1} & L_{n2} & \dots & L_{nn} \end{bmatrix} \begin{bmatrix} \lambda_1^{-1} & 0 & 0 & 0 \\ 0 & 0 & 0 & 0 \\ 0 & 0 & \dots & 0 \\ 0 & 0 & 0 & 0 \end{bmatrix}$$
$$\times \begin{bmatrix} T_{11} & T_{12} & \dots & T_{1n} \\ T_{21} & T_{22} & \dots & T_{2n} \\ \dots & \dots & \dots & \dots \\ T_{n1} & T_{n2} & \dots & T_{nn} \end{bmatrix} [I]$$
$$= \begin{bmatrix} \lambda_1^{-1}L_{11} & 0 & \dots & 0 \\ \lambda_1^{-1}L_{21} & 0 & \dots & 0 \\ \dots & \dots & \dots & \dots \\ \lambda_1^{-1}L_{n1} & 0 & \dots & 0 \end{bmatrix} \begin{bmatrix} T_{11} & T_{12} & \dots & T_{1n} \\ T_{21} & T_{22} & \dots & T_{2n} \\ \dots & \dots & \dots & \dots \\ T_{n1} & T_{n2} & \dots & T_{nn} \end{bmatrix} [I]$$
$$= \lambda_1^{-1} \begin{bmatrix} L_{11}T_{11} & L_{11}T_{12} & \dots & L_{11}T_{1n} \\ L_{21}T_{11} & L_{21}T_{12} & \dots & L_{21}T_{1n} \\ \dots & \dots & \dots & \dots \\ L_{n1}T_{11} & L_{n1}T_{12} & \dots & L_{n1}T_{1n} \end{bmatrix} \begin{bmatrix} I_1 \\ I_2 \\ \dots \\ I_n \end{bmatrix}. \tag{5}$$

The approximation is made possible because $1/\lambda_1$, the critical modal impedance, is much larger than the other modal impedances. The diagonal elements of the above matrix characterize the combined excitability and observability of the critical mode at the same bus. They are called participation factors of the bus to the critical mode. The definition is $PF_{bm} = L_{bm}T_{mb}$ where b is the bus number and m is the mode number.

It is worthwhile to point out that the eigen-analysis technique is not limited to systems of linear differential equations. They are applicable for any systems involving matrices. Eigen-analysis is essentially a matrix decoupling technique. Although eigen-analysis gained its recognition in the power system field when applied to dynamic stability analysis. Its most popular application is, however, the symmetrical component analysis. The concept of participation factors was introduced in [4]. It has been applied to analyze power system dynamic stability (differential equations) [5] and voltage stability (algebraic equations) [6] successfully in the past.

The resonance mode concepts presented above are illustrated with a simple system shown in Fig. 1. The per-unit frequency is based on the fundamental frequency and is equal to harmonic

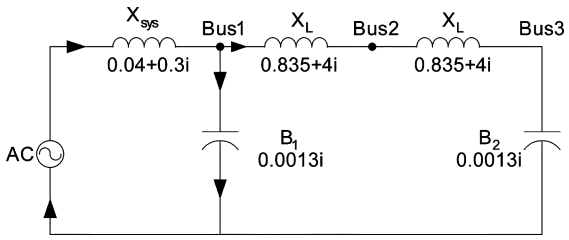

Fig. 1. Three-bus test system.

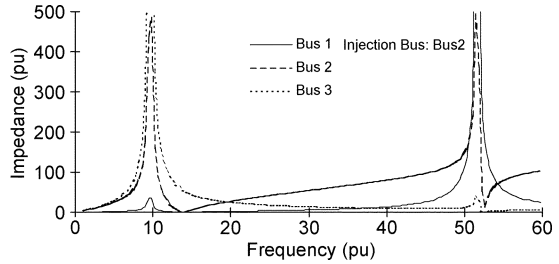

Fig. 2. Frequency scan results of the test system.

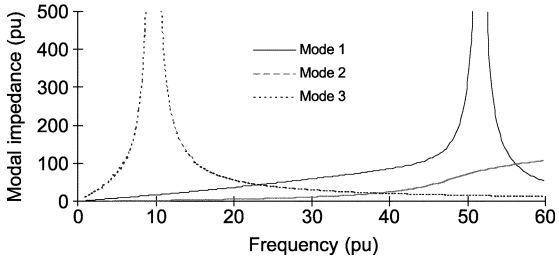

Fig. 3. Modal impedances of the test system.

number. There are three buses in the system where harmonic resonance could be excited or observed. Fig. 2 shows the bus frequency scan results when bus 2 is injected with 1.0-p.u. current. The results reveal that the resonance phenomenon can be observed at all three buses. It is therefore difficult to identify the significance of each bus in the resonance condition. The eigenvalue (or modal impedance) chart Fig. 3, on the other hand, shows that only one mode experiences resonance at a specific frequency. The mode 1 has a resonance frequency of 51.6 p.u. and mode 3 has a resonance frequency of 9.6 p.u.. Mode 2 does not experience resonance.

Table I documents the eigenvalues, eigenvectors and participation factors for the two critical modes. The results show that bus 1 has the largest eigenvector and participation factor values for the resonance mode 1. The key participating bus for mode 3 is bus 3. These conclusions can be verified by analyzing the parallel resonance circuits looking into the system from the key participating buses. For bus 1, capacitor B_1 is in parallel with X_{sys} ($2X_L$ is very large and can be ignored when paralleled with X_{sys}). The approximate resonance frequency is $f = \sqrt{X_c/X_{sys}} = 50.637$ p.u., which is very close to the mode 1 resonance frequency of 51.6 p.u. For bus 3, the capacitor B_2 is in parallel with the $X_{sys} + 2X_L$, the resonance frequency is $f = \sqrt{X_c/(X_{sys} + 2X_L)} = 9.633$ p.u., which coincides with the mode 3 resonance frequency of 9.6 p.u.. The results therefore confirm that the information provided by the

TABLE I
MODAL ANALYSIS RESULTS OF THE TEST SYSTEM

Resonance freq (pu)			9.6 (Mode 3)	51.6 (Mode 1)
Critical eigenvalue			0.00021/-10.08°	0.00015/-10.43°
Critical Eigen-Vectors	T	Bus 1	T_{31}=0.0332/0.60°	T_{11}=0.9002/-0.31°
		Bus 2	T_{32}=0.4605/0.15°	T_{12}=0.4344/0.51°
		Bus 3	T_{33}=0.8870/-0.11°	T_{13}=0.0338/-179.38°
	L	Bus 1	L_{13}=0.0332/0.68°	L_{11}=0.9001/0°
		Bus 2	L_{23}=0.4605/0.26°	L_{21}=0.4343/0.82°
		Bus 3	L_{33}=0.8870/0°	L_{31}=0.0338/-179.07°
Participation factor (mag.)		Bus 1	PF_{13}=0.0011	**PF_{11}=0.8103**
		Bus 2	PF_{23}=0.2121	PF_{21}=0.1887
		Bus 3	**PF_{33}=0.7868**	PF_{31}=0.0011

modal analysis can indeed reveal the locations easiest to excite or observe harmonic resonance.

III. CHARACTERISTICS OF RESONANCE MODES

Section II has provided the theoretical background for the proposed resonance mode analysis technique. Some interesting results have been obtained. There is a need to understand the characteristics of the indices further before the method can be used with confidence. The objective of this section is to fully investigate the characteristics of modal resonance.

A. Complex Y Matrix Versus Real Y Matrix

Complex admittance matrices and voltage/current vectors are employed to explain the resonance mode theory in Section II. The problem can also be formulated into a real matrix/vector problem by splitting the real and imaginary parts of the variables. In fact, many power system analysis programs use the real Y matrix formulation. The first step of our investigation is to determine the similarities and differences of the two formulations. The results will clarify which formulation is more suitable for the proposed technique. The real Y matrix formulation has the following form (for a 2-node system):

$$V_r = \begin{bmatrix} V_{1x} \\ V_{2x} \\ V_{1y} \\ V_{2y} \end{bmatrix} = Y_r^{-1} I_r$$

$$= \begin{bmatrix} G_{11} & G_{12} & -B_{11} & -B_{12} \\ G_{21} & G_{22} & -B_{21} & -B_{22} \\ B_{11} & B_{12} & G_{11} & G_{12} \\ B_{21} & B_{22} & G_{21} & G_{22} \end{bmatrix}^{-1} \begin{bmatrix} I_{1x} \\ I_{2x} \\ I_{1y} \\ I_{2y} \end{bmatrix}$$

where the subscripts "x" and "y" denote the real and imaginary parts of the phasors respectively. The subscript "r" indicates real matrix formulation. In this formulation, all quantities are real numbers. The system of Fig. 1 is used to compute the eigenvalues of both Y and Y_r matrices. To simplify the presentation of results, bus 2 of the system is eliminated so that there are two modes for the Y matrix and 4 modes for the Y_r matrix.

Fig. 4 shows loci of eigenvalues of the Y and Y_r matrices. The real matrix has four loci since its size is twice of the complex one. It can be seen that two of the loci are identical to those of the complex matrix. The other two are the conjugate images of the first two. The conclusion is that the Y_r formulation provides extra conjugate results for the eigenvalues. Table II lists the eigenvectors of the Y_r matrix at the resonance frequency of 9.6 p.u.

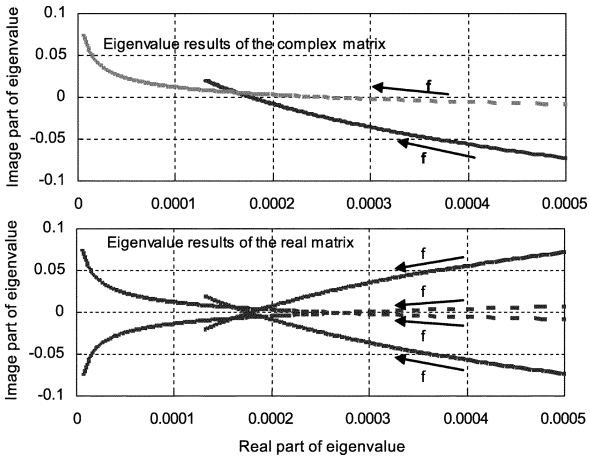

Fig. 4. Loci of eigenvalues of the test system.

TABLE II
MODAL INFORMATION DERIVED FROM THE Y_r MATRIX

Resonant freq (pu)			9.6 (Mode 3)	
Critical eigenvalue			0.00021/-10.08°	
			Associated with V_{ix}	Associated with V_{iy}
Critical Eigen-Vectors	T	Bus 1	T_{31}=0.0332/0.60°	T_{34}=0.0332/90.57°
		Bus 2	T_{32}=0.4605/0.15°	T_{35}=0.4605/90.15
		Bus 3	T_{33}=0.8870/-0.11°	T_{36}=0.8870/89.89°
	L	Bus 1	L_{13}=0.0332/0.68°	L_{43}=0.0332/-89.32°
		Bus 2	L_{23}=0.4605/0.26°	L_{53}=0.4605/-89.74°
		Bus 3	L_{33}=0.8870/0°	L_{63}=0.8870/-90°

It can be seen that results in Table II are redundant: the two sets have identical magnitudes. The eigenvectors associated with V_{ix} parts are conjugate of those with the V_{iy} parts. These conclusions are proven in the Appendix. The significance of these results is that they have clarified the modal relationship between the Y and Y_r matrices. It is useful for those who need to choice the Y matrix formulation for modal analysis.

B. Relationship Between the Left and Right Eigenvectors

According to (2), the eigenvalue and eigenvector are defined as follows:

$$[\Lambda] = [L]^{-1}[Y][L]. \tag{6}$$

Since $[Y] = [Y]^T$ and $[\Lambda]$ is a diagonal matrix, there is

$$\begin{aligned}[\Lambda] = [\Lambda]^T &= \left([L]^{-1}[Y][L]\right)^T \\ &= [L]^T A^T \left([L]^{-1}\right)^T = [L]^T A \left([L]^{-1}\right)^T. \end{aligned} \tag{7}$$

Comparing (6) and (7), one can conclude $[L]^{-1} = [L]^T$. Since $[T] = [L]^{-1}$, we have $[T] = [L]^T$, i.e. the left eigenvector is equal to the right eigenvector. This is a very important conclusion. It not only simplifies the proposed resonance mode analysis technique but also reveals the unique characteristics of harmonic resonance. Some of the interesting conclusions that can be deduced are:

- The bus that has the highest observability level (i.e., largest left eigenvector entry) for a mode is also the one that has the highest excitability level (i.e., largest right eigenvector entry). It implies that if a harmonic current matching the resonance frequency is injected into this bus, the bus will see the highest harmonic voltage level. If the current is injected into a different bus, the distortion level is likely to be amplified in the system.
- The participation factors are equal to the square of the eigenvectors. As a result, one index, eigenvector or participation factor, is sufficient for resonance mode analysis. The magnitude of the index characterizes how far the resonance will propagate. The bus with the highest participation factor can be considered as *the center of resonance*.

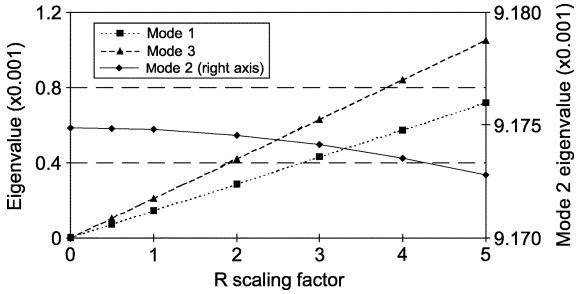

Fig. 5. Eigenvalues as functions of system resistance.

C. Ideal Resonance Condition

The proposed method was conceived from the reasoning that a sharp resonance is associated with a very small eigenvalue. An ideal resonance case is the one where the $[Y]$ matrix becomes singular. To verify this postulation, the 3-bus test system is modified by scaling its resistive components to zero in steps. The modal analysis results are shown in Fig. 5. It can be seen that two of the eigenvalues indeed approaches zero since there are two resonance modes. This will result in very sharp peaks of the frequency scan impedance curves. Note that the eigenvalues are functions of frequency as well. Fig. 5 shows the smallest eigenvalues in the frequency range from 1 to 60 p.u.

D. Critical Mode and "True" Resonance Frequency

In this paper, we define the minimum eigenvalue as the critical mode. Although called the critical mode, this eigenvalue must be sufficiently small to produce harmful resonance. The threshold to define "smallness" could be system dependent and could also be affected by the degree of conservativeness one decides to have. This is a subject worthy further investigation. What is of interest here is the frequency corresponding to the critical mode. We call this frequency the modal resonance frequency.

To demonstrate the importance of modal resonance frequency, the test system shown in Fig. 6 is used. This system has one capacitive element and is expected to have only one resonance frequency. The frequency scan analysis shown in Fig. 7, however, reveals that there appear two resonance frequencies in the system, although they are close. Resonance frequency is defined in this paper as the frequency where the impedance reaches its peak.

With the help of modal analysis, we can find that both resonance frequencies are actually associated with the same critical mode. The "true" resonance frequency is the one corresponding to the minimum eigenvalue. The reason that the frequency scan results show different resonance frequencies is due to the fact that the frequency scan impedances are the combined results of

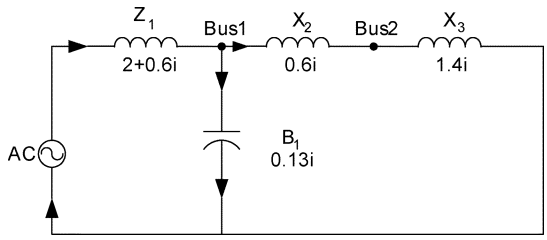

Fig. 6. Test system with one capacitive element.

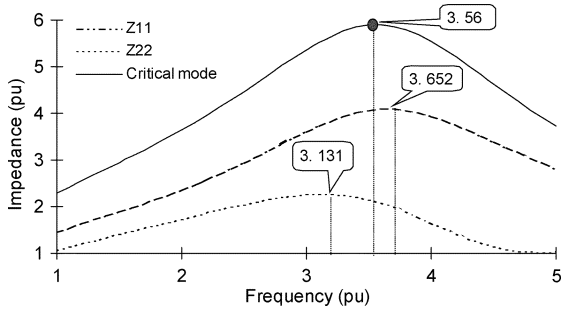

Fig. 7. Frequency responses of self- and modal impedances.

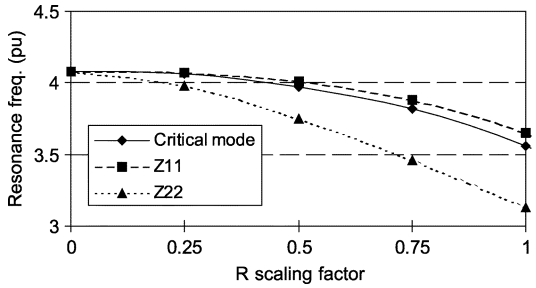

Fig. 8. Resonance frequencies as affected by resistances.

different modes. For example, the driving point impedance at bus 2 can be expressed as follows:

$$Z_{22} = \lambda_1^{-1} PF_{21} + \lambda_2^{-1} PF_{22} + \ldots + \lambda_n^{-1} PF_{2n} = Z_{m1} PF_{21} + Z_{m2} PF_{22} + \ldots + Z_{mn} PF_{2n} \quad (8)$$

where the first subscript of PF stands for the bus number and the second script for mode number. Since there are other terms in the above equation, maximum Z_{22} does not necessarily occur when λ_1 is the smallest. However, if the resistive components in the system are reduced sufficiently, λ_1 can become very small. The first term will dominate the value of Z_{22} and the resonance frequency of Z_{22} will approach the modal resonance frequency. Fig. 8 shows the impact of reducing the system resistance on the resonance frequency. It can be seen that when the resistance is reduced to zero, all resonance frequencies converge to the same value.

This finding has a significant implication for harmonic resonance analysis: although the frequency scan analysis may reveal different resonance frequencies, they could all relate to the same resonance phenomenon. It is the modal resonance frequency that can be considered as the "true" resonance frequency.

E. Series Resonance

In this paper, parallel resonance refers to the phenomenon where a small current injection to a bus will cause very large voltages in a system. It corresponds to the cases where $[Y]^{-1}$ has large values. Since most harmonic sources behave as current sources, parallel resonance is the main concern in harmonic analysis. The series resonance refers to the cases where a small voltage applied to a bus could lead to large branch currents. Series resonance can be observed when the impedance obtained from the frequency scan becomes very small. One may wonder if eigen-analysis can be used to the $[Z] = [Y]^{-1}$ matrix to identify the critical modes of series resonance. This problem is investigated by using the test system of Fig. 1.

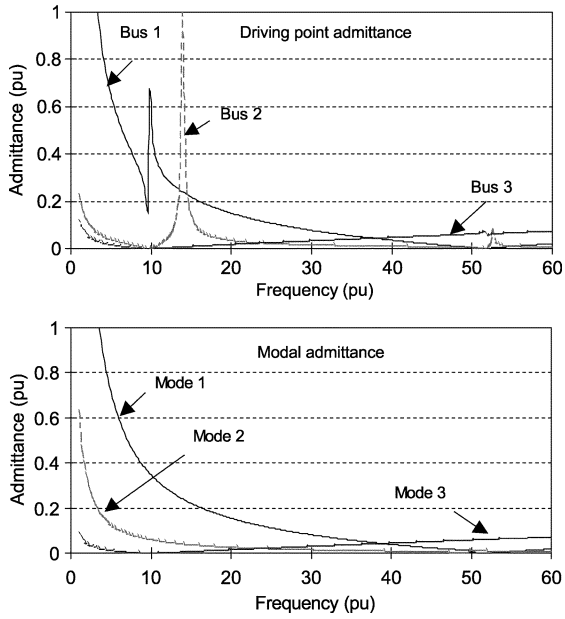

Fig. 9. System admittances.

The driving point admitances, defined as the inverse of the driving point impedances, are shown in the top chart of Fig. 9. They are in fact the Norton admittances seen at the bus. Large admittance is observed at around $f = 13$ p.u. Hence one series resonance point exists in this system. However, the inverse of the eigenvalues of the $[Z]$ matrix shown in the bottom chart doesn't have large values at the frequency.

This was a surprise finding. If one analyzes the problem further, however, the phenomenon becomes understandable. A series resonance means that the circuit has a loop with a very small loop impedance. If the loop is applied with a voltage, a large loop current will be produced. The correct formulation to identify series resonance should, therefore, be the $[\mathrm{Z_{loop}}]$ matrix defined in loop equation $[\mathrm{Z_{loop}}][\mathrm{I_{loop}}] = [\mathrm{E}]$.

IV. Verification and Sensitivity Studies

Two test systems have been used to evaluate the characteristics and applications of the resonance mode analysis technique. Due to space limitation, only shown here are the results of the IEEE-14 bus test system [7]. The one-line diagram of this system is available in Fig. 18.

A. Identification of the Critical Mode

According to the theory of Section II, it is easy to identify the "location" of harmonic resonance in the modal domain.

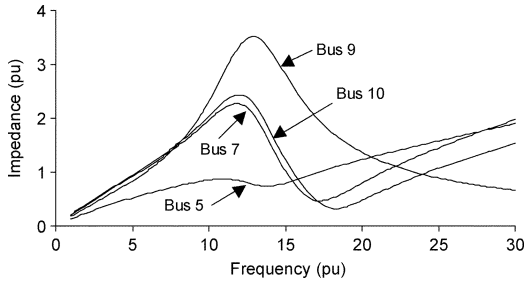

Fig. 10. Driving-point and transfer impedances.

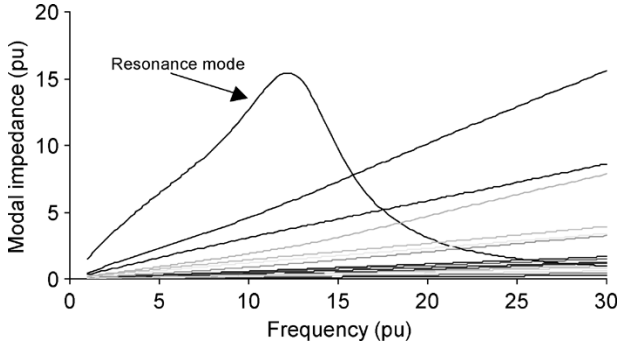

Fig. 11. Modal impedances.

This postulation is verified using the test system. The system is modified with only one capacitor left at Bus 9. So that "one-mode" resonance phenomenon can be seen. The results are shown in Figs. 10 and 11. The first figure shows some of the bus voltages of the test system when bus 9 is injected with 1.0 per-unit current. The results are essentially the driving-point and transfer impedances of the network. It can be seen that most impedances exhibit a resonance condition. So it is hard to identify the relative significance of each bus in the resonance condition. The modal impedance chart, on the other hand, shows that there is only one mode experiencing resonance. This is the mode associated with the capacitor. The participation factors confirmed this conclusion. Bus 9 is found to have the largest PF for the mode. If one solely relies on the frequency scan analysis, it would be difficult to find the key bus involved in the resonance.

B. Number of Resonance Modes

Harmonic resonance is caused by the energy exchange between the capacitive and the inductive elements in the system. If there were one capacitive element, one would expect to see one resonance mode. This has been confirmed in previous section. If there are two capacitive elements, at least two modes of resonance could be expected. The question is if there are more modes of resonance? For example, could two capacitors work together to resonate with the rest of the system? To clarify this point, three two-capacitor cases are investigated:

- **Case 1**: Two shunt capacitors. The two capacitors are connected to Buses 9 and 10 ($B = 0.0633$ and 0.0549 p.u., respectively). The modes in Fig. 12 have only two peaks even if the frequency range is up to 200th harmonic.
- **Case 2**: Two filters. Each filter has one capacitor. Different combinations of the two filters are tried: a) the 11th filters are at Buses 3 and 8 respectively and b) both filters are at Bus 3. The first combination shows two peaks. The second combination has only one peak because the two capacitors are identically connected to the same bus. They are equivalent to one single capacitor (Fig. 13).
- **Case 3**: Long transmission line with two charging shunts. The shunts of the branch between Buses 1 and 2 are kept and the mode shapes are plotted in Fig. 14. More than two peaks are observed for this case and the peaks repeat about every 50 harmonics. This phenomenon is attributed to the long line model employed for transmission lines. The line charging in this model varies with the harmonic order and is not a physical capacitor. As frequency increases, one would expect that more line shunts need to be added to represent the line accurately. So the number of resonance modes will increase.

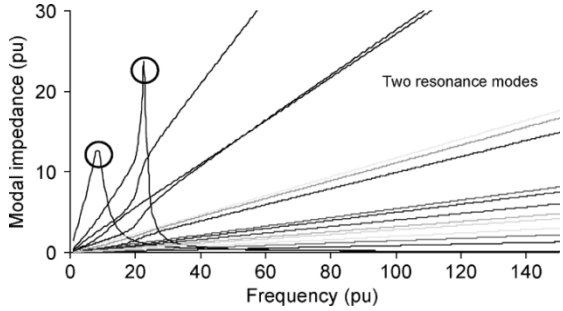

Fig. 12. Mode shapes of Case 1.

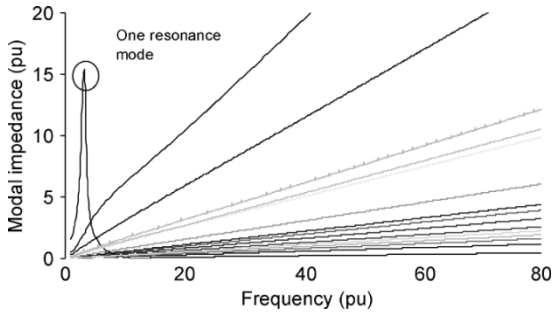

Fig. 13. Mode shapes of Case 2b.

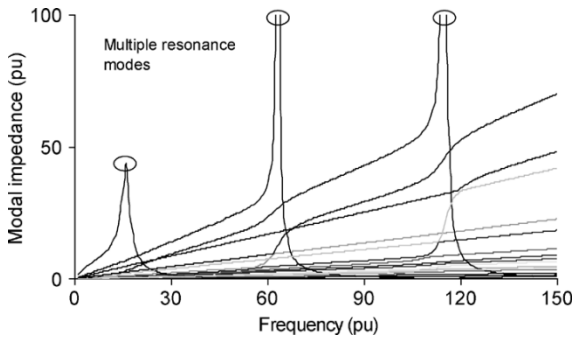

Fig. 14. Mode shapes of Case 3.

Three capacitor cases were also tested and three peaks were found in the mode shape plot. The results in this section suggest that the number of resonance modes is likely equal to the number of physical and equivalent (line shunt) capacitors for the harmonic frequency of practical interest (<50th, depending on

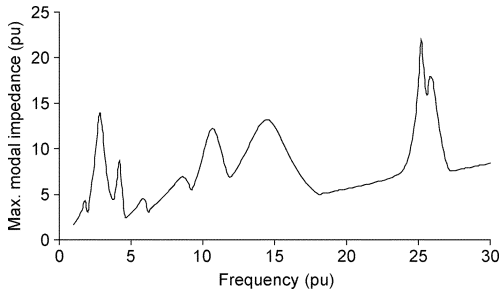

Fig. 15. Critical mode of the IEEE 14-bus system.

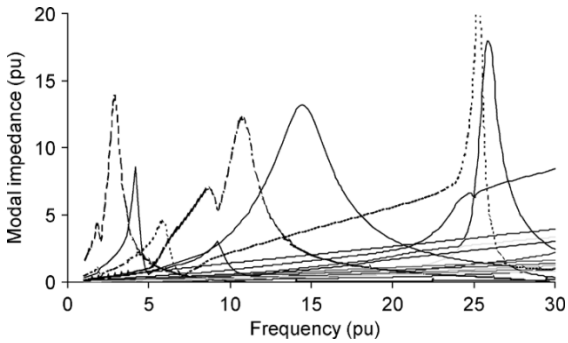

Fig. 16. Mode shapes of the IEEE-14 bus system.

TABLE III
RESONANCE MODE INFORMATION OF THE TEST SYSTEM

Modal resonance freq (pu)	Critical eigenvalues (magnitude)	Most part. bus	Least part. Bus
1.9	0.1835	8	6
2.8	0.0719	3	12
4.2	0.1163	8	1
5.9	**0.2207**	**8**	**2**
8.6	0.4408	9	3
10.7	**0.2186**	**1**	**3**
14.5	0.0758	9	3
25.3	**0.0452**	**2**	**14**
25.9	0.0554	1	2

line length). The resonance effects of the capacitors appear to be decoupled. Each capacitor contributes to one mode. There is no "joint" resonance mode involving more than one capacitor. The implication is that one only needs to identify a single capacitor to find the source of a resonance problem. This work can be easily done with the help of eigenvector or participation factor.

C. Full Case Studies

Resonance mode analysis has been conducted on the unmodified IEEE 14-bus system. The variation of the critical mode as a function of frequency is shown in Fig. 15. The critical mode is defined as the maximum modal impedance at any given frequency. It can be seen that there are 7 resonance peaks in the frequency range of 1 p.u. to 30 p.u. Fig. 15 is what one will get if a power iteration method (see Section IV-E) is used to calculate the critical mode. In order to understand the characteristics of the proposed method fully, we have traced each mode shape. The results are shown in Fig. 16. It can be seen that Fig. 15 shows the maximum value of the curves shown in Fig. 16.

Main modal information of the system is summarized in Table III. Due to space limitation, only three modes are selected

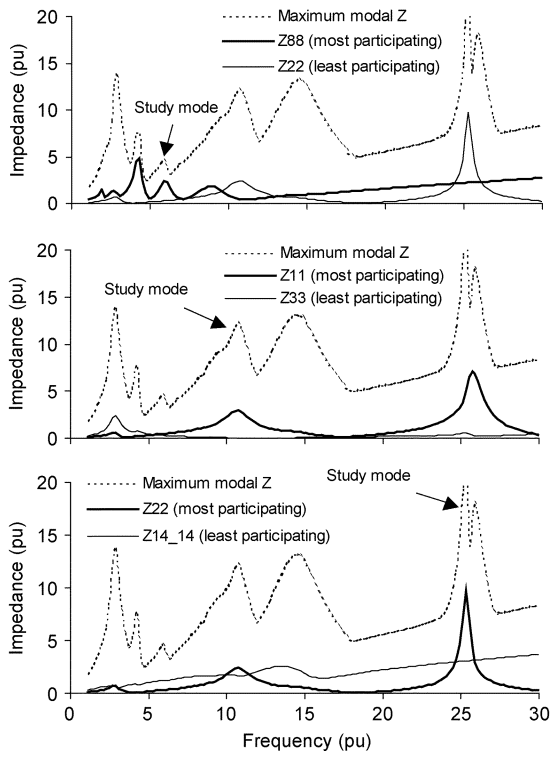

Fig. 17. Modal and driving-point impedances.

for detailed analysis. The driving point impedances of the most and least participating buses are calculated and shown in Fig. 17. This figure also includes the maximum modal impedance. It can be seen from this figure that the most participating buses have impedance peaks coinciding with the peaks of the modal impedances under study. The least participating buses do not exhibit any peak behavior at the resonance frequencies of the study modes. The results further confirm that participation factor is a good index to identify the location of resonance.

The impact area of the resonance can be seen from the bubble charts shown in Fig. 18. The sizes of the bubbles are in proportion to the participation factors. The system one-line diagram is shown at the background to assist the identification of mode locations. The center of each resonance mode can be clearly seen from the charts. It is found that resonance corresponding to modes $\mathrm{f} = 5.9$ p.u. and $\mathrm{f} = 25.3$ p.u. are limited to small areas while the resonance at $\mathrm{f} = 10.7$ p.u. affects large areas. The physical meaning of a mode that can affect a large area is still under investigation.

D. Weighted Participation Factor

The participation factors (and eigenvectors) are good at measuring the participation of different buses to a particular mode. It is also useful to have an index that can assess the degree of involvement of each bus in different modes. This index will facilitate the cross-mode comparison as well. For this purpose, the concept of weighted participation factor (WPF) is introduced as follows

$$\mathrm{WPF}_{bm} = \lambda_m^{-1} PF_{bm} = Z_m PF_{bm}$$

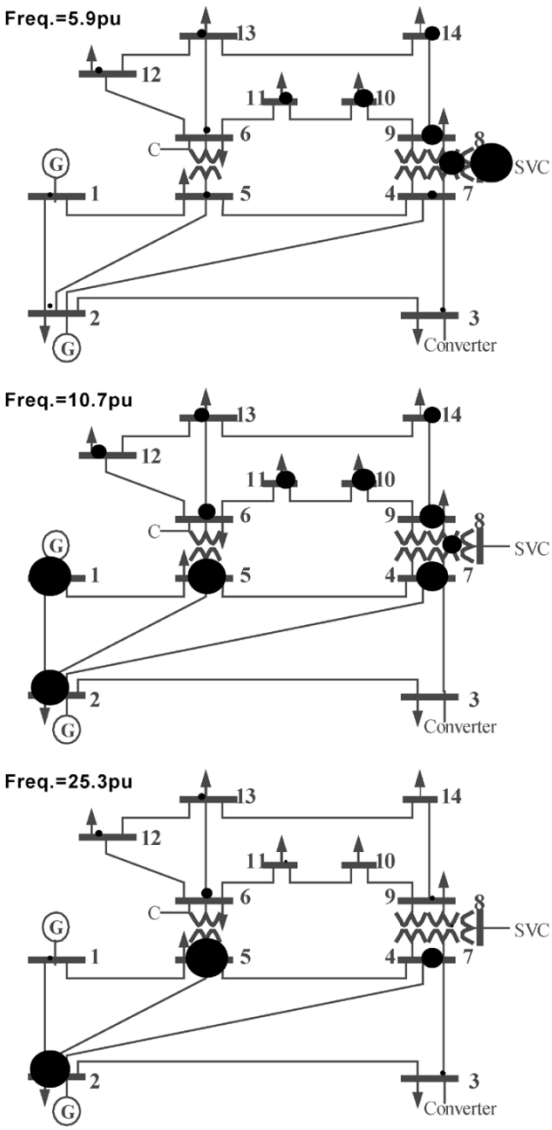

Fig. 18. Propagation or impact area of harmonic resonance.

where subscript b standards for bus number and m the mode number. The weighted PF includes the effect of Z_m. Since modal impedances for different modes can be compared, using Z_m as a weighting factor will make the cross-mode comparison of participation factors possible. According to (8), the driving point impedance of bus B can be expressed

$$Z_{bb} = WPF_{b1} + WPF_{b2} + \ldots + WPF_{bn}.$$

As a result, the weighted participation factor has a physical meaning as well. It is the portion of a driving- point impedance that is associated only with a particular mode.

E. Calculating the Critical Mode

Since the critical mode is the largest eigenvalue of the $[\mathrm{Y}]^{-1}$ matrix at a given frequency, we can use the simple 'power iteration' method to find the critical mode. 'Power iteration' method is a very effective tool to find the largest eigenvalue and its corresponding eigenvector for a matrix [3]. It works as follows:

1) Select an arbitrary starting vector V_o and set the iteration count $k = 1$;

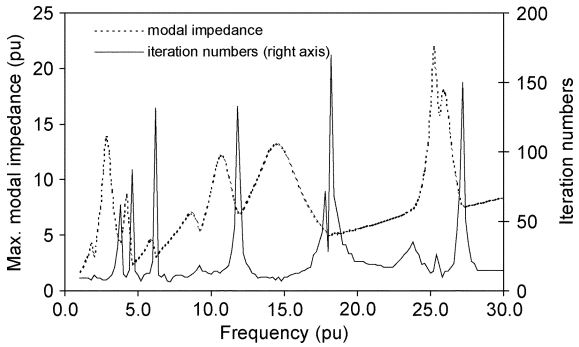

Fig. 19. Iteration numbers of the power iteration method.

2) Calculate $U_k = Y^{-1}V_{k-1}$;
3) Calculate $V_k = U_k/\|U_k\|_\infty$, where $\|U_k\|_\infty = \max(|u_{1_k}|, \ldots, |u_{1_k}|)$ is the largest element value of the U_k vector;
4) If $\|U_k\|_\infty - \|U_{k-1}\|_\infty \leq \varepsilon$, stop iteration and go to step 5; otherwise set $k = k + 1$ and go to step 2;
5) $|\lambda_1| \approx \|U_k\|_\infty$ and the corresponding eigenvector is V_k.

The power iteration method has been tested on the test system. The number of iterations needed to converge to an accuracy of 0.0001 is shown in Fig. 19. The critical mode shape is also shown. It is interesting to see that the number of iterations is about 20 around the resonance frequencies. The number gets much higher at the 'turning points' of the mode shape. This is because there are two or more eigenvalues with comparable values at those points. The power iteration method is known to take more iteration if the eigenvalues are close to each other. The results show that the task to find the critical mode (at the resonance frequencies) is not a very computing-intensive work.

V. Conclusion

In this paper, the phenomenon of harmonic resonance is investigated from the perspective of harmonic resonance modes. The results have revealed many interesting insights on the phenomenon. Based on the results a resonance mode analysis technique is proposed. The main findings of this work are of the following.

- Harmonic resonance is caused by the inherent characteristics of a network. The resonance actually takes place at a specific mode. It is not related to or caused by a particular bus current injection. The resonance mode can be found by calculating the smallest eigenvalue of the network admittance matrix.
- Harmonic current injections at certain buses can excite the resonance mode more easily than at other buses. These buses can be identified by examining the bus participation factors (or eigenvector entries) associated with the resonance mode. The factors characterize the impact area of the resonance. The bus with the highest participation factor is the center of the resonance. The bus with the highest excitability for a mode is also the one with the highest observability for the mode.
- The case study results reveal that the number of resonance mode is likely equal to the number of physical and equivalent (line shunt) capacitors. The capacitive

elements' effect on resonance appears to be decoupled. Each capacitor contributes to one mode. There is no "joint" resonance mode involving more than one capacitor. The implication is that one only needs to identify a single capacitive element to find the source of a resonance problem.

The proposed modal analysis method is a new tool for harmonic resonance assessment. There are two schemes to use the method to assist harmonic analysis:

1) Critical mode scan based modal analysis: In this scheme, the power iteration method is implemented at every step of the frequency scan process. A maximum modal impedance (i.e. the critical mode) versus frequency curve is obtained. The peaks of the curve are identified. For those peaks that are close to harmonic frequencies, the participation factors are examined to determine the center and impact area of the resonance.
2) Frequency scan based modal analysis: In this scheme, traditional frequency scan analysis is conducted first. If the results show potentially harmful resonance points, these points will be analyzed further by using the resonance mode analysis technique. The modal information will reveal the critical mode and its impact area. Since the peak of traditional frequency scan curve does not necessarily coincide with the true resonance frequency, resonance mode analysis should be conducted in a range around the resonance point identified by the frequency scan analysis.

APPENDIX

For a general power system, the real and complex admittance matrices have the following mathematical expression

$$\mathbf{Y_r} = \begin{bmatrix} \mathrm{Re}(\mathbf{Y}) & -\mathrm{Im}(\mathbf{Y}) \\ \mathrm{Im}(\mathbf{Y}) & \mathrm{Re}(\mathbf{Y}) \end{bmatrix} = \begin{bmatrix} \frac{\mathbf{Y}+\mathbf{Y}^*}{2} & -\frac{\mathbf{Y}-\mathbf{Y}^*}{j2} \\ \frac{\mathbf{Y}-\mathbf{Y}^*}{j2} & \frac{\mathbf{Y}+\mathbf{Y}^*}{2} \end{bmatrix}$$

where superscript "*" demotes conjugate operation. Substituting the modal decomposition, [L][Λ][T], of [Y] into the above equation yields

$$\begin{aligned} \mathbf{Y_r} &= \begin{bmatrix} \frac{L\mathbf{\Lambda}\mathbf{T}+L^*\mathbf{\Lambda}^*\mathbf{T}^*}{2} & -\frac{L\mathbf{\Lambda}\mathbf{T}-L^*\mathbf{\Lambda}^*\mathbf{T}^*}{j2} \\ \frac{L\mathbf{\Lambda}\mathbf{T}-L^*\mathbf{\Lambda}^*\mathbf{T}^*}{j2} & \frac{L\mathbf{\Lambda}\mathbf{T}+L^*\mathbf{\Lambda}^*\mathbf{T}^*}{2} \end{bmatrix} \\ &= \begin{bmatrix} \frac{L}{\sqrt{2}} & \frac{L^*}{\sqrt{2}} \\ \frac{-jL}{\sqrt{2}} & \frac{jL^*}{\sqrt{2}} \end{bmatrix} \begin{bmatrix} \mathbf{\Lambda} & 0 \\ 0 & \mathbf{\Lambda}^* \end{bmatrix} \begin{bmatrix} \frac{\mathbf{T}}{\sqrt{2}} & \frac{j\mathbf{T}}{\sqrt{2}} \\ \frac{\mathbf{T}^*}{\sqrt{2}} & \frac{-j\mathbf{T}^*}{\sqrt{2}} \end{bmatrix} \end{aligned}$$

The above equation is the eigen-decomposition of the $\mathbf{Y_r}$ matrix. It can be seen that there is redundant information in the matrices: the eigenvalues and eigenvectors corresponding to the real part of the phasors have a conjugate relationship with those associated with the imaginary part of the phasors.

REFERENCES

[1] CEA Technology Inc., "Impact of Harmonics on Utility Equipment: A Survey and Review of Published Work," Tech. rep., Rep. no. T024 700-5117, Nov. 2003.

[2] IEEE Harmonics Model and Simulation Task Force, "Modeling and simulation of the propagation of harmonics in electric power networks: part I," *IEEE Trans. Power Del.*, vol. 11, no. 1, pp. 466–474, Jan. 1996.

[3] R. Bellman, *Introduction to Matrix Analysis*, 2nd ed. New York: McGraw-Hill, 1970.

[4] I. J. Perez-Arriaga, G. C. Verghese, and F. C. Schweppe, "Selective modal analysis with applications to electric power systems—I. Heuristic introduction," *IEEE Trans. Power App. Syst.*, vol. PAS-101, no. 9, pp. 3117–3125, Sep. 1982.

[5] ——, "Selective modal analysis with applications to electric power systems—II. The dynamic stability problem," *IEEE Trans. Power App. Syst.*, vol. PAS-101, no. 9, pp. 3126–3134, Sep. 1982.

[6] P. Kundur, *Power System Stability and Control*. New York: McGraw-Hill, 1994.

[7] IEEE Harmonics Model and Simulation Task Force, "Test systems for harmonics modeling and simulation," *IEEE Trans. Power Del.*, vol. 14, no. 2, pp. 579–587, Apr. 1999.

Wilsun Xu (M'90–SM'95) received the Ph.D. degree from the University of British Columbia, Vancouver, BC, Canada, in 1989.

Currently he is a Professor with the University of Alberta, Edmonton, AB, Canada. He was an Engineer with BC Hydro, Vancouver, BC, Canada, from 1990 to 1996. His main research interests are power quality and harmonics.

Zhenyu Huang (M'01) received the B.Eng. degree from Huazhong University of Science and Technology, Wuhan, China, in 1994, and the Ph.D. degree from Tsinghua University, Beijing, China, in 1999.

From 1998 to 2002, he conducted research at McGill University and the University of Alberta as a Postdoctoral Fellow, and at the University of Hong Kong. He is currently a development engineer at the Pacific Northwest National Laboratory, Richland, WA. His research interests include power electronics, power system stability and power quality.

Yu Cui received the B.Eng. degree from Tsinghua University, Beijing, China in 1995; the M.Sc. degree from the Institute of Electrical Engineering, Chinese Academy of Sciences, Beijing, China in 2000; and the M.Sc. degree from University of Saskatchewan, Canada, in 2003. He is currently pursuing the Ph.D. degree at the University of Alberta, Edmonton, AB, Canada.

His research areas include power quality and power system stability.

Haizhen Wang received the B.Sc.degree from the Shandong University, China in 1999 and the M.Sc. degree from the University of Alberta, Edmonton, AB, Canada, in 2003.